Inorg. Chem. **2007**, *46*, 4809–4814

Synthesis and Characterization of Low-Coordinate Divalent Aryl Transition-Metal Halide Analogues of Grignard Reagents: Precursors for Reduction to Metal–Metal-Bonded Complexes

Andrew D. Sutton,[†] Tailuan Ngyuen,[†] James C. Fettinger,[†] Marilyn M. Olmstead,[†] Gary J. Long,[‡] and Philip P. Power*,[†]

Department of Chemistry, One Shields Avenue, University of California, Davis, California 95616, and Department of Chemsitry, University of Missouri−Rolla, Rolla, Missouri 65409

Received June 20, 2006

The synthesis and characterization of the series of divalent first-row aryl transition-metal(II) halide compounds $[Cr(\mu\text{-}Cl)Ar']_2$ (**1**) and $(Li(OEt_2)Ar'MI_2]_2$ (M = Mn (**2**), Fe (**3**), and Co (**4**); Ar′ = C_6H_3-2,6-(C_6H_3-2,6-^{i}Pr$_2$)$_2$) are described. **1**–**4** were prepared by the addition of one equiv of Ar′Li to the respective transition-metal dihalides. They were characterized by UV–vis spectroscopy, magnetic measurements, and by X-ray crystallography. In dimeric **1**, each chromium center has quasi-four-coordinate, square-planar geometry, in which the metal is terminally bound to a terphenyl ligand through the ipso carbon of the central ring and to two bridging chloride ligands. There is a further interaction between chromium and an ipso carbon from one of the flanking –C_6H_3-2,6^{i}Pr$_2$ rings. In contrast, for the iodo derivatives **2**–**4**, LiI is not eliminated upon addition of LiAr′ to MI_2. Instead, the diethyl ether solvated adducts, $[Li(OEt_2)Ar'MI_2]_2$ (M = Mn (**2**), Fe (**3**), or Co (**4**)) were isolated. These possess a distorted cubane $Li_2M_2I_4$ core, in which the lithiums are bound to an ether and the transition metals are bound to a terphenyl group. Magnetic measurements between 2 and 300 K reveal the expected weak antiferromagnetic exchange coupling in each of the complexes.

Introduction

Recent work has shown that several main-group terphenyl derivatives of the type ArMMAr (M = Al−Tl, Ge−Pb; Ar = terphenyl) that have formal M−M multiple bonds can be synthesized and characterized.[1−4] Their stability depends on the use of the large terphenyl ligand Ar′ = C_6H_3-2,6(C_6H_3-2,6-^{i}Pr$_2$)$_2$,[5] and their synthesis was usually effected via the reduction of terphenyl-metal-halide precursors.[6] Although the major justification for these investigations has been the study of new metal−metal bonds, the structures and properties of their terphenyl-halide precursors are also of significant interest and have been the subject of several investigations.[7−9] In contrast, heteroleptic transition-metal halide species of the formula Ar′MX and Ar′MX$_2$ have received little attention and only a handful of examples have been well characterized. These include $[Co(\mu\text{-}Br)Ar^{\#}(THF)]_2$,[10] (Ar$^{\#}$ = (−C_6H_3-2,6-(C_6H_3-2,4,6-CH_3)$_2$), and the closed shell species (Et_2O)Li-(ICuAr′).[11] There are, however, other related heteroleptic transition-metal halide species that are based on different sterically large ligands such as the β-diketiminate derivatives [({(2,6-^{i}PrC_6H_3)N^{t}BuC}$_2$CH)MCl] (M = Ni,[12] Co[12] and Fe[13])

* To whom correspondence should be addressed. E-mail: pppower@ucdavis.edu.
[†] University of California, Davis.
[‡] University of Missouri−Rolla.

(1) Stender, M.; Phillips, A. D.; Wright, R. J.; Power, P. P. *Angew. Chem., Int. Ed.* **2002**, *41*, 1785−1787.
(2) Wright, R. J.; Phillips, A. D.; Hino, S.; Power, P. P. *J. Am. Chem. Soc.* **2005**, *127*, 4794−4799.
(3) Pu, L.; Twamley, B.; Power, P. P. *J. Am. Chem. Soc.* **2000**, *122*, 3524−3525.
(4) Phillips, A. D.; Wright, R. J.; Olmstead, M. M.; Power, P. P. *J. Am. Chem. Soc.* **2002**, *124*, 5930−5931.
(5) Schiemenz, B.; Power, P. P. *Angew. Chem., Int. Ed.* **1996**, *35*, 2150−2152.
(6) Pu, L.; Phillips, A. D.; Richards, A. F.; Stender, M.; Simons, R. S.; Olmstead, M. M.; Power, P. P. *J. Am. Chem. Soc.* **2003**, *125*, 11626−11636.
(7) Simons, R. S.; Pu, L.; Olmstead, M. M.; Power, P. P. *Organometallics* **1997**, *16*, 1920.
(8) Pu, L.; Twamley, B.; Power, P. P. *Organometallics* **2000**, *19*, 2874.
(9) Eichler, B. E.; Pu, L.; Stender, M.; Power, P. P. *Polyhedron* **2001**, *20*, 551.
(10) Ellison, J. J.; Power, P. P. *J. Organomet. Chem.* **1996**, *526*, 263−267.
(11) Hwang, C. S.; Power, P. P. *J. Organomet. Chem.* **1999**, *589*, 234−238.
(12) Holland, P. L.; Cundari, T. R.; Perez, L. L.; Eckert, N. A.; Lachicotte, R. J. *J. Am. Chem. Soc.* **2002**, *124*, 14416−14424.

10.1021/ic061121o CCC: $37.00
Published on Web 05/10/2007

and [({(2,6-^{i}PrC$_6$H$_3$)NMeC}$_2$CH)Mn(I)(THF)].[14] In addition, there are the recently described heteroleptic thiolates of the type [^{t}Bu$_3$SiSMX]$_n$ (M = Fe, Co, X = Cl, n = 12; M = Fe, Ni, X = Br, n = 12; M = Fe, X = I, n = 14)[15,16] We showed recently that the reduction of the heteroleptic chromium(II) species, Ar′CrCl with KC_8 gave the Cr(I)−Cr(I) dimer Ar′CrCrAr′, in which the chromium atoms were linked through a 5-fold bonding interaction.[17] We were therefore anxious to characterize the Ar′CrCl precursor and to isolate and further characterize examples of heteroleptic Ar′MX (M = first-row transition metal, X = halide) Grignard-like species as potential candidates for reduction to give metal−metal-bonded species. We now report the synthesis of the series of metal(II) aryl halides [Cr(μ-Cl)Ar′]$_2$ (**1**) and [Li(OEt$_2$)Ar′MI$_2$]$_2$ (M = Mn (**2**), Fe (**3**), or Co (**4**)). In addition, we describe their characterization by X-ray crystallography, electronic and ^{1}H NMR spectroscopy, and magnetic measurements.

Experimental Section

General Procedures. All of the manipulations were carried out using modified Schlenk techniques under an argon atmosphere or in a Vacuum Atmospheres HE-43 drybox. All of the solvents were dried over an aluminum column and degassed three times (freeze−thaw) prior to use. (LiAr′)$_2$ was prepared according to a literature procedure.[5] $CrCl_2(THF)_2$ was prepared by literature methods,[18] and CoI_2 (Cerac) was used as received. The iodides MnI_2 and FeI_2 (Aldrich) were further purified before use by washing the crude salts with benzene to remove any excess iodine. ^{1}H NMR spectra were recorded on a Varian 300 MHz instrument and referenced to the residual protio benzene in the C_6D_6 solvent. Melting points were recorded in glass capillaries sealed under N_2 or Ar and are uncorrected. UV−vis data were recorded on a Hitachi-1200 spectrometer. Attempts to obtain C, H analytical data gave inconsistent results probably because of partial desolvation.

[Cr(μ-Cl)Ar′]$_2$·*n*-hexane (1·*n*-hexane). (LiAr′)$_2$ (1.62 g, 2.0 mmol) in Et$_2$O (25 mL) was added dropwise to a stirred solution of $CrCl_2(THF)_2$ (1.07 g, 4.0 mmol) in Et$_2$O (25 mL) with cooling to ca. 0 °C. The resulting blue solution was allowed to warm to room temperature and was stirred overnight. The solvent was removed under reduced pressure, and the resulting blue solid was extracted with hexanes (30 mL). The solution was filtered and concentrated to ca. 5 mL under reduced pressure, which afforded royal blue X-ray-quality crystals of **1**·*n*-hexane after storage for 24 h at ca. −20 °C. Yield 1.36 g (70%), mp = 115−119 °C. ^{1}H NMR (300 MHz, C_6D_6, 25 °C, δ): 7.2 (s, br), 2.7 (s, br), 1.0 (s, br). UV (hexanes) λ_{max}, nm (ϵ, mol^{-1} L cm^{-1}) 677 (200).

[Li(OEt$_2$)Ar′MnI$_2$]$_2$·*n*-hexane (2·*n*-hexane). (LiAr′)$_2$ (1.62 g, 2.0 mmol) in Et$_2$O (25 mL) was added dropwise to a stirred suspension of MnI_2 (1.23 g, 4.0 mmol) in Et$_2$O (25 mL) with cooling in an ice bath. The resulting pale-yellow solution was allowed to warm to room temperature and was stirred overnight. The solvent was removed under reduced pressure, and the resulting light-brown solid was extracted with toluene (30 mL) and filtered. The volume was reduced to ca. 5 mL, which afforded pale-pink X-ray-quality crystals of **2**·*n*-hexane after 1 day at −20 °C. Yield 2.84 g (56%), mp = 270 °C (dec). ^{1}H NMR (300 MHz, C_7D_8, 25 °C, δ): 7.20 (br, s), 2.9 (br, s), 1.2 (br, s). UV (toluene) λ_{max}, nm (ϵ, mol^{-1} L cm^{-1}) 296 (3100), 334 (2100).

[Li(OEt$_2$)Ar′FeI$_2$]$_2$·*n*-hexane (3·*n*-hexane). (LiAr′)$_2$ (1.62 g, 2.0 mmol) in Et$_2$O (25 mL) was added dropwise to a stirred suspension of FeI_2 (1.24 g, 4.0 mmol) in Et$_2$O (25 mL) with cooling in an ice bath. The resulting dark-red solution was allowed to warm to room temperature and stirred was overnight. The solvent was removed under reduced pressure, and the resultant dark-red solid was extracted with hexanes (30 mL) and filtered. The volume was reduced to ca. 5 mL, and storage at ca. −20 °C for 3 days afforded deep-red X-ray-quality crystals of **3**. Yield 2.02 g (61%), mp = 265 °C (dec). ^{1}H NMR (300 MHz, C_6D_6, 25 °C, δ): 43 (br, s), 29.3 (br, s), 12.9 (br, s), 9.6 (br. s), 7.4 (br, s), 3.6 (br, s), −6.2 (br, s), −14.0 (br, s), −19.4 (br, s), −25.4 (br, s), −35.8 (br, s), −38.1 (br, s), −41.3 (br, s), −52.5 (br, s). UV (hexanes) λ_{max}, nm (ϵ, mol^{-1} L cm^{-1}) 394 (7800).

[Li(OEt$_2$)Ar′CoI$_2$]$_2$·*n*-hexane (4·*n*-hexane) (LiAr′)$_2$ (1.62 g, 2.0 mmol) in Et$_2$O (25 mL) was added dropwise to a stirred suspension of CoI_2 (1.25 g, 4.0 mmol) in Et$_2$O (25 mL). The resulting green solution was allowed to warm to room temperature and stirred overnight. The solvent was removed under reduced pressure, and the resultant green solid was extracted with hexanes (30 mL) and filtered. The volume was reduced to ca. 5 mL, which afforded emerald-green X-ray-quality crystals upon overnight storage at −20 °C. Yield 1.93 g (58%), mp = 160−163 °C. ^{1}H NMR (300 MHz, C_6D_6, 25 °C, δ): 14.1 (br, s), 9.3 (br, s), 3.1 (br, s). UV (toluene) λ_{max}, nm (ϵ, mol^{-1} L cm^{-1}) 294 (6100), 334 (5100), 790 (850).

X-ray Crystallographic Studies. Suitable crystals of the hexane solvates **1**−**4** were selected and covered with a layer of hydrocarbon oil under a rapid flow of argon. They were mounted on a glass fiber attached to a copper pin and placed in the cold N_2 stream on the diffractometer. X-ray data were collected on a Bruker SMART 1000 diffractometer at 90(2) K using Mo Kα radiation (λ = 0.71073 Å) or on a Bruker SMART Apex II diffractometer at 90(2) K with Mo Kα radiation (λ = 0.71073 Å). Absorption corrections were applied using SADABS.[19] The structures were solved using direct methods and refined by the full-matrix least-squares procedure in SHELX.[20] All of the non-hydrogen atoms were refined anisotropically, whereas hydrogens were placed at calculated positions and included in the refinement using a riding model.

Magnetic Studies. The samples for magnetization measurements wre sealed under N_2 in 3 or 4 mm quartz tubing. The sample magnetization was measured using a Quantum Design MPMSXL7 superconducting quantum interference device (SQUID) magnetometer. For each measurement, the sample was zero-field cooled to 5 K, and the magnetization was measured as a function of field to 2 T. The field was then reduced to 1 T, and the magnetization of the sample was measured in 0.5 K increments to 4 K, 1 K increments to 10 K, 2.5 K increments to 60 K, and 10 K increments to 320 K.

(13) Smith, J. M.; Lachicotte, R. J.; Holland, P. L. *Chem. Commun.* **2001**, 1542−1543.
(14) Chai, J.; Zhu, H.; Most, K.; Roesky, H. W.; Vidovic, D.; Schmidt, H.-G.; Noltemeyer, M. *Eur. J. Inorg. Chem.* **2003**, 4332−4337.
(15) Sydora, O. L.; Wolczanski, P. T.; Lobkovsky, E. B. *Angew. Chem., Int. Ed.* **2003**, *42*, 2685−2687.
(16) Sydora, O. L.; Henry, T. P.; Wolczanski, P. T.; Lobkovsky, E. B.; Rumberger, E.; Hendrickson, D. N. *Inorg. Chem.* **2006**, *45*, 609−626.
(17) Nguyen, T.; Sutton, A. D.; Brynda, M.; Fettinger, J. C.; Long, G. J.; Power, P. P. *Science* **2005**, *310*, 844−847.
(18) Job, R.; Earl, R. *Inorg. Nucl. Chem.* **1979**, *15*, 81−83.
(19) *SADABS*, version 5.0 package; an empirical absorption correction program from the SAINTPlus NT; Bruker AXS: Madison, WI 1998.
(20) SHELXL, version 5.1; Bruker AXS: Madison WI 1998.
(21) Chai, J.; Zhu, H.; Stueckl, A. C.; Roesky, H. W.; Magull, J.; Bencini, A.; Caneschi, A.; Gatteschi, D. *J. Am. Chem. Soc.* **2005**, *127*, 9201−9206.
(22) Borras, J. J.; Clemente, J. M. *J. Comput. Chem.* **2001**, *22*, 985−991.

Results and Discussion

Synthesis and Spectroscopy. Recent work has shown that low-valent transition-metal halide derivatives related to the target compounds, Ar′MX, could be synthesized by using sterically hindering bidentate β-diketiminate ligands to afford complexes such as [({2,6-^{i}Pr$_2$C$_6$H$_3$)N(^{t}Bu)C}$_2$CH)MCl] (M = Ni,[12] Co[12], and Fe[13]) and [({2,6-^{i}Pr$_2$C$_6$H$_3$)N(Me)C}$_2$CH)-Mn(I)]$_2$.[14] The latter species can be reduced with potassium metal to afford the Mn−Mn singly bonded complex (N−N)MnMn(N−N) (N−N = {(2,6-^{i}Pr$_2$C$_6$H$_3$)N(Me)C}$_2$CH),[21] in which the manganese atoms are coordinated by two nitrogens from the β-diketiminate ligands. However, in order to prepare species in which the multiple metal−metal bonding is maximized, the coordination number must be minimized in order to maintain the largest-possible number of metal d orbitals available for metal−metal bonding. This requirement can be met by using bulky monodentate ligands, such as Ar′, which can both maintain a low-coordination number at the metal center and stabilize the requisite metal-halide precursors. **1**−**4** were synthesized in good yield (ca. 60−70%) by simple addition of one equiv of Ar′Li to the respective metal dihalide at low temperature to afford a series of air- and moisture-sensitive complexes. The preparation of [Cr(μ-Cl)Ar′]$_2$ (**1**) proceeded smoothly with complete elimination of LiCl to yield blue crystals of the product in 70% yield (eq 1). Extension of this synthetic protocol to include late transition-metal analogues has not yet led to products with sufficient crystal quality for X-ray crystallography. In contrast, the use of M(II) iodides led to the formation of the cubanes **2**−**4**, which are formed by the inclusion of LiI in the product (eq 2) as shown by X-ray crystallography. To date, none of the complexes have displayed a tendency to undergo equilibria involving diarylmetal species. Our investigations have shown that both types of complexes are suitable precursors for new metal−metal-bonded species exemplified by the synthesis and characterization of a Ar′CrCrAr′ complex with an unprecedented Cr−Cr bond formed by a quintuple orbital interaction.[17]

$$2CrCl_2(THF)_2 + 2Ar'Li \xrightarrow{Et_2O,\ 0\ °C} \underset{\mathbf{1}}{[Cr(\mu\text{-}Cl)Ar']_2} + LiCl \quad (1)$$

$$2MI_2 + 2Ar'Li \xrightarrow{Et_2O,\ 0\ °C} [Li(OEt_2)Ar'MI_2]_2 \quad (2)$$

M = Mn (**2**), Fe (**3**), Co (**4**)

The UV−visible spectra of **1**−**4** are characterized by intense absorptions below 250 nm corresponding to $\pi-\pi^*$ transitions within the terphenyl ligand. In addition, **1** and **3** exhibit low-intensity absorptions centered at 677 nm (ϵ = 200 mol^{-1} L cm^{-1}) and 790 nm (ϵ = 850 mol^{-1} L cm^{-1}), respectively, corresponding to Laporte forbidden d−d transitions. Also, **3** and **4** have bands located at 394 (ϵ = 7800 mol^{-1} L cm^{-1}) and 334 nm (ϵ = 5100 mol^{-1} L cm^{-1}) respectively. **2** has a featureless spectrum in the visible region, which is expected for a high-spin d^5 system.

Magnetism. Magnetic susceptibility studies were carried out on crystalline samples of **1**−**4** to evaluate the extent, if any, of the magnetic exchange within the dimeric complexes. The temperature dependence of the molar magnetic susceptibility of the manganese(II) dimer, **2**, is shown in Figure 1; the corresponding inverse molar magnetic susceptibility is linear above ca. 150 K and yields a Weiss temperature of −90 K; below 50 K, the inverse molar susceptibility increases dramatically. Both the maximum in the susceptibility observed at ca. 45 K, (Figure 1), and the negative Weiss temperature are consistent with the expected presence of weak antiferromagnetic Mn(II)−Mn(II) exchange in **2**. Thus, the magnetic susceptibilities have been fit with the standard-exchange vector-coupled model[22−25] (see Supporting Information for details of the Hamiltonian used) with g = 2.00 as would be expected for this high-spin 3d^5 manganese(II) ion. Initial fits indicated that the molar susceptibility at the lowest temperatures was somewhat higher than predicted by the exchange model presumably because of traces of a paramagnetic Mn(II) or Mn(III) monomer. Thus, a paramagnetic contribution to the molar magnetic susceptibility with J = 0 cm^{-1} was included in the fits. A least-squares fit to the observed molar magnetic susceptibility of **2** leads to a virtually perfect fit, the black line in Figure 1, with an exchange coupling constant of $J = -6.57 \pm 0.02$ cm^{-1}, the green line, and a 1.3% contribution, the red line, from the paramagnetic impurity. The rather-small negative J value is reasonable for **2**, in which the superexchange through iodides I1 and I2 involves two 87.04(5)° Mn−I−Mn bond angles; little or no exchange would be expected for a 90° bond angle.

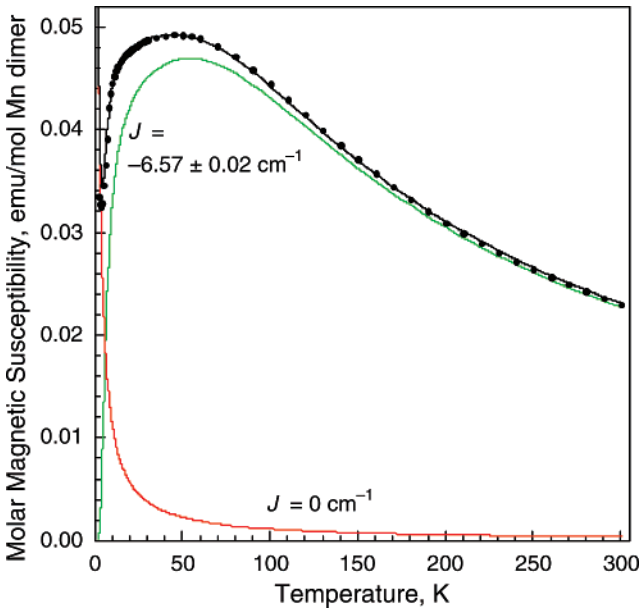

Figure 1. Temperature dependence of the molar magnetic susceptibility of [Li(OEt$_2$)Ar′MnI$_2$]$_2$, **2**. The black line corresponds to the total fit comprising the antiferromagnetically coupled dimer, green line, and a trace of paramagnetic impurity, red line.

(23) Zeigler, H. J., Pratt, G. W. *Magnetic Interaction In Solids;* Clarendon Press: Oxford, 1973.
(24) Martin, R. L. In *New Pathways In Inorganic Chemistry;* Ebsworth, E. A. V., Maddock, A. G., Sharpe, A. G., Eds.; Cambridge University Press: Cambridge, 1968, p 175.
(25) Kahn, O. *Molecular Magnetism;* VCH Publishers: New York, 1993, pp 38−43.

Table 1. Selected Crystallographic Data and Collection Parameters for **1**−**4**

	1·*n*-hexane	2[a]	**3**·*n*-hexane	**4**·*n*-hexane
formula	$C_{66}H_{88}Cr_2Cl_2$	$C_{68}H_{94}Mn_2I_4Li_2O_2$	$C_{74}H_{108}Fe_2I_4Li_2O_2$	$C_{74}H_{108}Co_2I_4Li_2O_2$
fw	1056.26	1574.79	1662.78	1668.94
color, habit	blue, prism	pale yellow, block	dark red, plate	green, plate
cryst syst	monoclinic	monoclinic	monoclinic	monoclinic
space group	$P2_1/n$	$P2_1/c$	$P2_1/c$	$P2_1/c$
a, Å	11.919(1)	14.487(5)	14.438(3)	14.426(2)
b, Å	20.682(2)	22.018(6)	22.045(4)	21.985(3)
c, Å	12.489(1)	25.736(8)	26.090(5)	25.938(4)
α, deg	90	90	90	90
β, deg	98.55(1)	104.23(3)	105.86(7)	105.77(8)
γ, deg	90	90	90	90
V, Å^3	3044.6(5)	7957(4)	7988(2)	7916.7(19)
Z	2	4	4	4
d_{calcd}, Mg/m^3	1.152	1.314	1.383	1.400
θ range, deg	1.92−31.5	1.23−27.48	1.23−27.48	1.23−27.48
μ, mm^{-1}	0.482	1.904	1.947	2.017
obs data, $I > 2\sigma(I)$	9572	18 238	18 290	18 139
R1 (obs data)	0.0848	0.0967	0.0367	0.0380
wR2 (all data)	0.2566	0.2570	0.1001	0.1124

[a] *n*-hexane is not included in the formula because of extensive desolvation.

The temperature dependence of the molar magnetic susceptibility of **1**, see Figure S1 in the Supporting Information, is rather similar to that shown in Figure 1; the corresponding inverse molar magnetic susceptibility is linear above ca. 100 K and yields a Weiss temperature of −100 K, and below ca. 60 K the inverse molar susceptibility increases dramatically. Again, both the maximum in the susceptibility observed at ca. 40 K, see Figure S1, and the negative Weiss temperature are consistent with weak antiferromagnetic Cr(II)−Cr(II) exchange, and the magnetic susceptibility has been fit as discussed above for **2**. An acceptable least-squares fit leads to an exchange coupling constant of $J = -7.0 \pm 0.1$ cm^{-1} and ca. 2% of a paramagnetic impurity. In this case, the fit at the lowest temperatures is not perfect, presumably because some portion of the impurity may be a Cr(III)−Cr(III) exchange-coupled dimer. However, again the rather-small negative *J* value is reasonable for **1**, in which the superexchange through Cl involves two 88.61(4)° Cr−Cl−Cr bond angles.

The temperature dependence of the molar magnetic susceptibility of **4**, see Figure S2, is somewhat similar to that shown in Figure 1 except that the peak corresponding to the Néel point is narrower and shifted down to 10 K; the corresponding inverse molar magnetic susceptibility is linear above ca. 150 K and yields a Weiss temperature of −342 K; below 150 K the inverse molar susceptibility first decreases and then increases below 10 K (see the inset to Figure S2). As is often the case for polynuclear cobalt(II) complexes, a determination of the magnetic exchange present in **4** required the inclusion of a large pseudo-zero-field splitting for the nominal $^4A_{2g}$ ground state of cobalt(II) in a low-symmetry environment. The best fit obtained for the molar magnetic susceptibility of **4** observed between 2 and 60 K (see Figure S3) yields a *g* of 1.90, a zero-field splitting, *D*, of ca. −100 cm^{-1}, and an exchange coupling constant, *J*, of ca. −1 cm^{-1}; values that are typical of cobalt(II) in the low-symmetry environment found in **4**. Rather surprisingly, in **4**, which has a Co−I−Co bond angle of 85.58(2)°, the antiferromagnetic exchange coupling is weaker than in **2**, which has a Mn−I−Mn bond angle of 87.04(5)°, a value that is closer to 90°.

Table 2. Selected Bond Lengths (angstroms) and Angles (deg) for **1**

		Cr(1)−Cl(1)−Cr(1A)	88.61(4)
Cr(1)−Cl(1)	2.375(2)	Cl(1)−Cr(1)−Cl(1A)	91.39(4)
Cr(1)−Cl(1A)	2.417(3)	C(6)−C(1)−Cr(1)	142.0(3)
C(1)−Cr(1)	2.041(3)	C(2)−C(1)−Cr(1)	99.9(2)
C(7)−Cr(1)	2.435(3)	C(1)−Cr(1)−Cl(1)	100.20(9)
Cr(1)−Cr(1A)	3.301(2)	C(1)−Cr(1)−Cl(1A)	167.9(1)
		C(1)−Cr(1)−C(7)	65.0(1)

The magnetic properties of **3** resemble those of a paramagnetic iron cluster, see Figure S4, and are similar to those observed for $[Fe(\mu\text{-Br})(\mu\text{-SSi}^t\text{Bu}_3)]_{12}$.[15,16] The inverse molar magnetic susceptibility of **3** is linear above 70 K and yields a Weiss temperature of −36 K, a Curie constant of 4.38 mol Fe/(emu K), and a corresponding μ_{eff} per iron of $5.92\mu_B$. The latter value seems to indicate that in spite of careful handling of the complex the iron(II) expected in **3** has been oxidized to iron(III). However, it should be noted that the molar magnetic susceptibility of **3** is also rather consistent[12,13] with the presence of high-spin iron(II) with a small *J* value of ca. −0.05 cm^{-1}, a *g* of ca. 2, and a large iron(II) zero-field splitting, *D*, of ca. −20 to −40 cm^{-1}. Although the fit is far from perfect and poorer than that shown in Figure S3, it is possible that **3** has not been or has only been partially oxidized to iron(III).

Structures. Important data collection and refinement parameters for **1**−**4** are provided in Table 1, and selected structural data are given in Tables 2 and 3. The structures of **1**−**4** are illustrated by those shown in Figures 2 and 3, respectively.

The structure of **1** is dimerized through bridging of the chromium atoms by chlorides and is characterized by an inversion center midway between the metals. The central Cr_2Cl_2 unit is planar with Cr−Cl−Cr and Cl−Cr−Cl angles of 88.61(4) and 91.39(4)°, respectively. The chromium atom is bound terminally to a C(1) (or C(1A)) ipso carbon of the central aryl ring of the terphenyl ligand (Cr(1)−C(1) =

(26) Edema, J. J. H.; Gambarotta, S.; Van Bolhuis, F.; Smeets, W. J. J.; Spek, A. L.; Chiang, M. Y. *J. Organomet. Chem.* **1990**, *389*, 47−59.

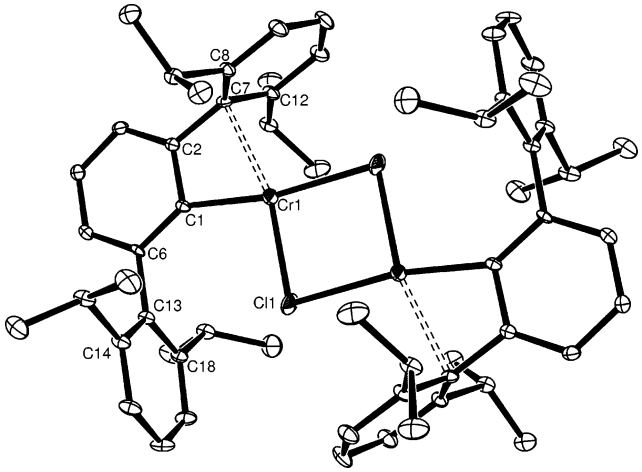

Figure 2. Thermal ellipsoid (30%) plot of [Ar′Cr(μ-Cl)]$_2$·*n*-hexane (**1**·*n*-hexane) (Ar′ = C_6H_3-2,6-(C_6H_3-2,6-^{i}Pr$_2$)$_2$)). Hydrogen atoms and hexane molecules are not shown.

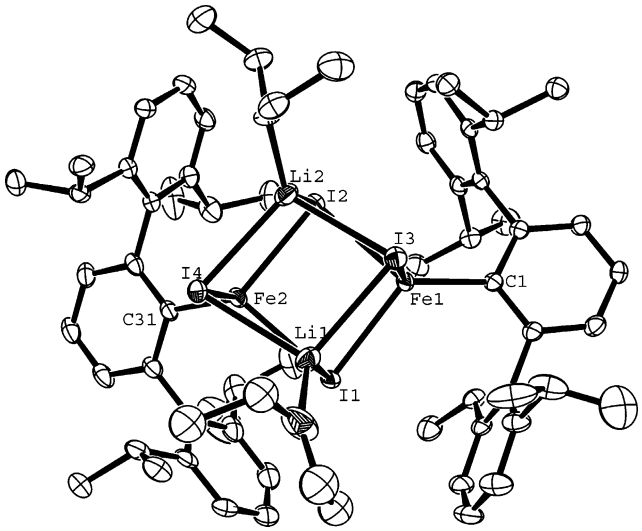

Figure 3. Thermal ellipsoid (50%) plot of [Li(OEt$_2$)Ar′FeI$_2$]$_2$·hexane (**3**·*n*-hexane) (Ar′ = C_6H_3-2,6-(C_6H_3-2,6-^{i}Pr$_2$)$_2$)). Hydrogen atoms are not shown.

2.041(3) Å) as well as to the two bridging chlorides (Cr−(μ-Cl) = 2.375(2) and 2.417(3) Å). The Cr−C bond length is slightly shorter than those in [Mes$_2$Cr(THF)$_2$].THF[26] (2.083(11) Å) and [Mes$_2$Cr(bipy)][26] (2.098(14) Å). However, there is an additional interaction with an ipso carbon (Cr-(1)−C(7) = 2.435(3) Å) of one of the flanking C_6H_3-2,6-^{i}-Pr$_2$ rings of the terphenyl group and the metal, which is more than 0.4 Å longer than that to the ipso carbon. Thus, the chromium can be considered to have a quasi-four-coordinate, square-planar environment rather than a three-coordinate geometry. The interaction of the chromium and the flanking aryl ring (attached to C(2) of the central ring) is also evident in the distortion of the bond angles at the ipso carbon. Thus, the Cr−C(1)−C(2) bond angle (99.9(2)°) is over 40° narrower than the Cr−C(1)−C(6) angle (142.0(3)°), presumably a result of the Cr(1)−C(7) interaction. The bridging Cr−Cl bond lengths are almost equal, and they are within range of the reported Cr−Cl bond lengths for the dichromium(II) complex [(DDP)Cr(μ-Cl)]$_2$ (DDPH = 2-{(2,6-diisopropylphenyl)amino}-4-{(2,6-diisopropylphenyl)imino}-pent-2-ene) (2.3877(9) and 2.3851(9) Å)[27] and similar to those in [{HC(PPh$_2$NSiMe$_3$)$_2$}Cr(μ−Cl)]$_2$ (2.405(2) and 2.437(1) Å).[28]

Table 3. Selected Bond Lengths (angstroms) and Angles (deg) for **2**−**4**

	2	**3**	**4**
M(1)−I(1)	2.793(5)	2.734(2)	2.675(6)
M(1)−I(2)	2.847(2)	2.776(9)	2.714(2)
M(1)−I(3)	2.819(2)	2.754(1)	2.692(1)
M(1)−C(1)	2.109(1)	2.044(3)	1.998(5)
M(2)−I(1)	2.847(2)	2.772(1)	2.709(2)
M(2)−I(2)	2.811(4)	2.748(9)	2.691(1)
M(2)−I(4)	2.813(8)	2.755(7)	2.691(4)
M(2)−C(31)	2.091(1)	2.038(4)	2.004(5)
C(1)−M(1)−I(1)	124.2(3)	123.61(9)	122.40(1)
C(1)−M(1)−I(2)	128.0(3)	128.18(10)	126.41(1)
C(1)−M(1)−I(3)	111.5(3)	110.26(9)	108.87(1)
C(31)−M(2)−I(1)	123.7(3)	124.94(10)	124.10(1)
C(31)−M(2)−I(2)	126.8(3)	124.99(11)	122.86(1)
C(31)−M(2)−I(4)	113.5(3)	111.04(10)	110.01(1)
M(1)−I(1)−M(2)	87.04(5)	86.79(3)	85.58(2)
M(1)−I(2)−M(2)	86.70(6)	86.40(6)	85.18(2)
I(1)−M(1)−I(2)	92.77(6)	92.59(2)	99.14(2)
I(1)−M(2)−I(2)	92.39(6)	92.38(2)	92.84(2)

2−**4** were synthesized by the reaction of the metal diiodide with one equiv of Ar′Li. The expected byproduct, LiI, does not separate. Instead, it remains incorporated in the structure even upon extraction with hexane. **2**−**4** are isostructural and isomorphous and adopt a heterocubane structure consisting of two transition metals, M (M = Mn (**2**), Fe (**3**), or Co (**4**)), and two lithium and four iodine atoms. Each transition metal is four-coordinate and is bound terminally to a carbon (C(1)) from a terphenyl group and three bridging iodines. The lithiums are also four-coordinate and are bound to three bridging iodines and a diethyl ether donor molecule. No further interactions between the metals and the terphenyls are apparent. The bond lengths involving the transition-metal decrease in the sequence Mn > Fe > Co and are in agreement with the decrease in size of these metals.[29]

For **2**, the Mn−C bond lengths are essentially equal (2.11-(1) and 2.09(1) Å) and are similar to those in the homoleptic Mn(II) derivatives [Mn(Mes*)$_2$] (Mes* = C_6H_2-2,4,6-^{t}Bu$_3$) (2.108(2) Å)[30,31] and [Mn{C(SiMe$_3$)$_2$}$_2$] (2.102(4) Å).[32] No further interactions between the metal center and the flanking aryl rings of Ar′ are apparent. The Mn−I bonds are in the narrow range of 2.793(2) to 2.847(2) Å and are slightly longer than those in the β-diketiminato complex [HC{(Me)C-(2,6-^{i}Pr$_2$H$_3$C$_6$N)}$_2$Mn(μ-I)$_2$Li(OEt$_2$)$_2$][33] (2.7354(9) and 2.7230-(9) Å) and in [(HC{(Me)C(2,6-^{i}Pr$_2$H$_3$C$_6$)$_2$N}Mn(μ-I)]$_2$[14] (2.7688(7) and 2.7484(8) Å). The Li−I bond lengths range from 2.778(19) to 2.899(19) Å with the longer bonds corresponding to iodides involved in bridging to the manganese centers. These Li−I bond lengths are similar to those

(27) Gibson, V. C.; Newton, C.; Redshaw, C.; Solan, G. A.; White, A. J. P.; Williams, D. J. *Eur. J. Inorg. Chem.* **2001**, 1895−1903.
(28) Wei, P.; Stephan, D. W. *Organometallics* **2002**, *21*, 1308−1310.
(29) Emsley, J. *The Elements;* Oxford University Press: Oxford, 1998.
(30) Wehmschulte, R. J.; Power, P. P. *Organometallics* **1995**, *14*, 3264−3267.
(31) Mueller, H.; Seidel, W.; Goerls, H. *Angew. Chem., Int. Ed.* **1995**, *34*, 325−327.
(32) Buttrus, N. H.; Eaborn, C.; Hitchcock, P. B.; Smith, J. D.; Sullivan, A. C. *Chem. Commun.* **1985**, 1380−1381.
(33) Prust, J.; Most, K.; Muller, I.; Stasch, A.; Roesky, H. W.; Uson, I. *Eur. J. Inorg. Chem.* **2001**, 1613−1616.

in the β-diketiminate complexes[14,33] (2.817(8) and 2.920(9) Å). The internal angles of the heterocubane core range from 79.7(6) (Li(1)−I(3)-Li(2)) to 100.4(6)° (I(4)−Li(1)-I(3)), illustrating the distortion in the heterocubane structure.

The Fe−C bond lengths in **3** (2.044(3) and 2.038(4) Å) are similar to the Fe−C bonds in the Fe(II) aryl [Fe(Mes*)$_2$] (2.058(6) Å).[30,31] The Fe−I bonds are in the range of 2.7341-(7) to 2.7769(7) Å and are similar to the Fe−I bond lengths in [{Ph$_3$PSFeI(μ-I)}$_2$][34] (2.732 and 2.644 Å). As in **2**, the Li−I bonds are in the range of 2.772(7) to 2.831(7) Å with the longer bonds involving iodides bridging the two iron atoms. These Li−I bond lengths are comparable to those in [{(Et$_3$N)LiI}$_4$][35] (2.822(6) to 2.840(6) Å), which has a central Li$_4$I$_4$ core. The heterocubane core has internal angles between 78.93(13) (Fe(2)−I(2)-Li(2)) and 101.699(19)° (I(2)−Fe(2)-I(4)), a similar range for **2**.

The structure of **4** closely resembles those of **2** and **3**. The Co−C bond lengths are equivalent (1.998(5) and 2.004(5) Å) and the Co−I bonds are in the range of 2.6755(7) to 2.7141(8) Å, which is also seen for [{Ph$_3$POCoI(μ-I)}$_2$][36] (2.647 and 2.652 Å). The Li−I bonds between 2.768(9) and 2.853(10) Å resemble those in [{(Et$_3$N)LiI}$_4$][35] (2.822(6) to 2.840(6) Å). As with **2** and **3**, the longer Li−I bonds involve coordination to the bridging iodide. The internal angles of the heterocubane core lie between 77.73(19) and 104.33-(2)° and show the largest range of such angles in the series **2**−**4**.

Conclusions

A series of first-row transition-metal aryl halides have been prepared by the reaction of the respective transition-metal dihalides with the bulky terphenyl lithium reagent Ar′Li (Ar′ = C$_6$H$_3$-2,6-(C$_6$H$_3$-2,6-^{i}Pr$_2$)$_2$). These species represent some of the first well-characterized divalent organo transition-metal halide complexes. Their isolation underlines the stabilizing influence of the large terphenyl ligands

Acknowledgment. We thank the donors of the Petroleum Research Fund administered by the American Chemical Society for financial support and Peter Klavins for assistance in magnetization measurements.

Supporting Information Available: Magnetic susceptibility plots of **1**, **3**, and **4**. Hamiltonian used for the determination of the exchange coupling in **2**. ^{1}H NMR spectra of **1**−**4**. This material is available free of charge via the Internet at http://pubs.acs.org.

IC061121O

(34) Saak, W.; Haase, D.; Pohl, S. *Z. Naturforsch., B: Chem. Sci.* **1988**, *43*, 289−294.
(35) Doriat, C.; Koeppe, R.; Baum, E.; Stoesser, G.; Koehnlein, H.; Schnöckel, H. *Inorg. Chem.* **2000**, *39*, 1534−1537.
(36) Gorter, S.; Hinrichs, W.; Reedijk, J.; Rimbault, J.; Pierrard, J. C.; Hugel, R. P. *Inorg. Chim. Acta* **1985**, *105*, 181−186.